ACS APPLIED MATERIALS & INTERFACES

www.acsami.org

Research Article

In Situ Generation of Regularly Ordered 2D Ultrathin Covalent Organic Framework Films for Highly Sensitive Photoelectrochemical Bioanalysis

Tingting Liu, Lin Cui,* Huijuan Zhao, and Xiaomei Zhang*

Cite This: https://dx.doi.org/10.1021/acsami.0c15147

Read Online

ACCESS | Metrics & More | Article Recommendations | Supporting Information

ABSTRACT: Developing new photoactive materials and electrode preparation technology with high stability, repeatability, easy fabrication, and a low electron−hole recombination rate is promising for ideal photoelectrochemical (PEC) biosensors, but it remains a great challenge. Here, a porous and crystalline oriented two-dimensional (2D) ultrathin covalent organic framework film (D-TA COF film) was formed *in situ* on indium-doped tin oxide (ITO) substrates under very mild conditions. The structure and morphology of D-TA COF film were characterized by means of Raman spectroscopy, X-ray photoelectron spectroscopy, scanning electron microscopy, and powder X-ray diffraction. Compared with the randomly oriented D-TA COF powder drop-coated on ITO, the photocurrent of the D-TA COF film grown on the ITO surface *in situ* achieved as high as ~333-fold increase. This photocurrent can be further amplified by O_2 (acting as electron acceptors). Benefiting from the fabrication *in situ*, D-TA COF film also exhibited tough adhesion, assuring the film was difficult to separate from the electrode. Accordingly, D-TA COF film was applied as the photoactive material to build a PEC biosensor for H_2O_2 detection based on coupling with large amounts of catalase (CAT) through simple adsorption. The introduced CAT catalyzed the decomposition of H_2O_2 to O_2, leading to an enhancement of the photocurrent response. As a result, a "signal-on" PEC biosensor was fabricated with good sensitivity, rapid response, and high stability, and it can also detect H_2O_2 released from living cells. Taking into account these advantages, the D-TA COF film is expected to be an ideal photoactive material to construct various PEC biosensors, which as far as we know have not been reported.

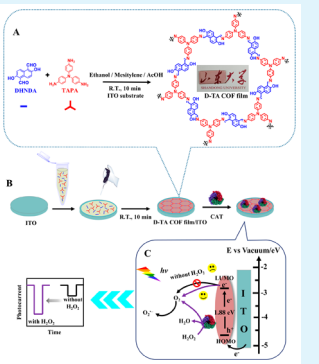

KEYWORDS: *covalent organic frameworks (COFs), ultrathin film, in situ generation, photoelectrochemical bioanalysis, dual signal amplification*

1. INTRODUCTION

Photoelectrochemical (PEC) bioanalysis is an innovative and promising methodology for detecting biomolecules.[1−3] In comparison with electrochemical and optical technologies, photoelectrochemistry naturally integrates their merits. It has higher sensitivity as well as a lower background signal because of the completely separated energy forms of the excitation source (light) and the detection signal (current).[4−6] The performance of PEC methods is not only closely related to the charge separation in photoactive materials at the electrode upon light irradiation but also relies on the charge mobility toward the respective electrode. The drop-coating method is still the widely adopted strategy to fabricate electrodes.[7−11] However, the unrepeatability and instability of photoactive materials on the electrode seriously preclude the charge mobility and in turn the PEC sensing applications. In addition, the lower photoelectric conversion efficiency and susceptibilities to photobleaching of common photoactive materials also limit the development of PEC sensing.[12] To overcome these limitations, new photoactive materials and electrode preparation technology need to be explored.

As a burgeoning crystalline material with a periodic structure and intrinsic porosity, covalent organic frameworks (COFs) have received increasing attention. They have great development potential in drug delivery,[13] separation,[14] gas adsorption,[15,16] catalysis,[17,18] and chemosensors.[19] COFs have also attracted ever-increasing attention as photoactive materials.[20,21] Their extensive π-conjugated structure endows the materials with unique optical and electrical properties. The tailorable pore size allows the transmission of suitable guest species. The high specific surface area provides an ample interface for charge separation. The highly ordered structure offers a conductive pathway for carrier transformation. These in conjunction with the larger electrostatic coupling and charge delocalization caused by the highly ordered stacking mode

Received: August 22, 2020
Accepted: September 25, 2020

Scheme 1. (A) Schematic Diagrams of the Preparation Process of D-TA COF Film and a Photograph of the D-TA COF Film on ITO (Inset); (B) Fabrication Process of the PEC Biosensor for H_2O_2 Detection; and (C) Photogenerated Electron Transfer Mechanism of the Strategy

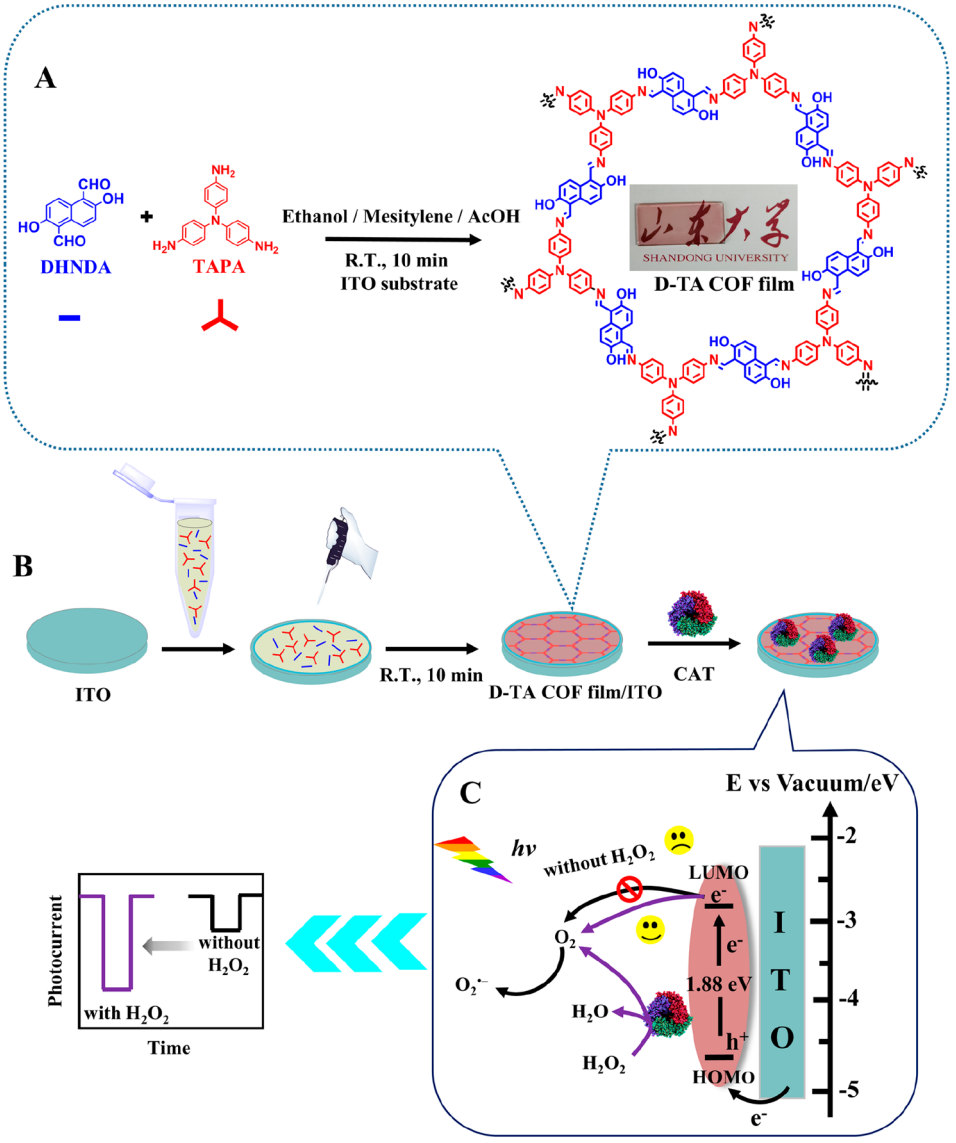

enable the materials to have excellent carrier mobility.[22] Benefiting from these unique properties, COF materials could hold significant promise as photoactive materials for PEC bioanalysis.

However, to implement bulk COF materials on electrodes still faces two challenges: (i) It is difficult to fabricate macro-ordered COF structures because of the uncontrolled coating methods, which affect their electron conduction performance.[23] (ii) The formed films can easily peel off the electrode due to their large particle size. These as well as traditionally harsh synthetic conditions, such as high temperature, high pressure, and overlong reaction times, seriously limit COFs sensing application. Recently, a few surface-mediated strategies have been explored to fabricate two-dimensional (2D) ordered COF films.[24−26] These films are nanometer thick ordered structures and can be grown on various substrates, such as indium-doped tin oxide (ITO), single-layer graphene, or even glass substrates. Compared with the disordered film fabricated from the COF materials, the 2D ordered COF films have more superior photoelectric properties due to their more ordered stacking mode.[27] Some functionalized COF materials have been utilized in several sensing modes, including colorimetric sensing,[28] fluorescent sensing,[29,30] and electrochemical sensing.[31] However, to our knowledge, investigation of bulk COFs as photoactive materials for PEC bioanalysis was only done once[32] and did not utilize 2D ordered COF films.

Hydrogen peroxide (H_2O_2) exists in various living organisms. It participates in numerous biological processes and mediates the physiological balance.[33] Abnormal levels of H_2O_2 in cells cause serious damage to proteins and DNA and in turn induce some diseases, such as neurodegeneration,[34] Alzheimer's disease,[35] diabetes,[36] and tumors.[37] Therefore, great efforts should be made to develop effective methods to accurately and effectively detect H_2O_2 in living cells. Diverse analytical methods including fluorescence,[38] colorimetry,[39] electrochemistry,[40,41] and photoelectrochemistry[42] have proved effective to probe H_2O_2. Among them, photoelectrochemical sensing with outstanding photoactive materials

https://dx.doi.org/10.1021/acsami.0c15147
ACS Appl. Mater. Interfaces XXXX, XXX, XXX−XXX

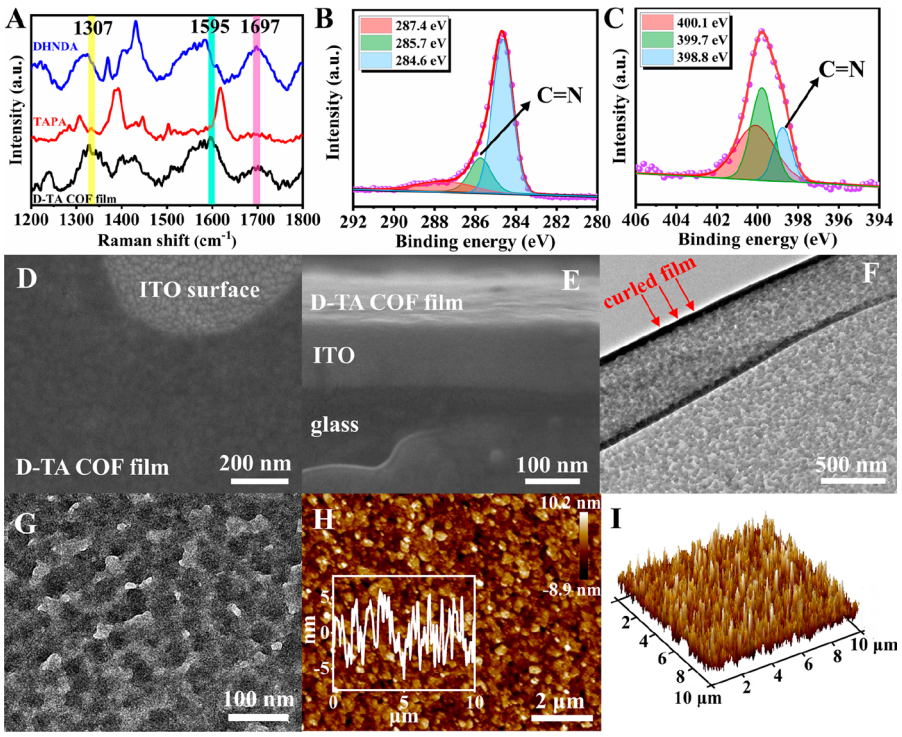

Figure 1. (A) Raman spectra of DHNDA, TAPA, and D-TA COF film. The high-resolution XPS spectra of C 1s (B) and N 1s (C) of D-TA COF film. SEM top view (D) and cross section (E) of D-TA COF film grown on the ITO. TEM images of D-TA COF film grown on the carbon-coated copper grid (F, G). AFM 2D (H) and AFM 3D (I) images of D-TA COF film on ITO.

and *in situ* generation of electron donors or acceptors as dual signal amplification have attracted substantial attention due to their high sensitivity and fast response.

On the basis of these considerations, we present a versatile strategy to *in situ* fabricate ultrathin covalent organic framework film (D-TA COF film) on ITO within a few minutes in air (Scheme 1A). The obtained D-TA COF film has a porous and inherent-ordered graphene-like multilayer structure. Benefiting from these features as well as the *in situ* growth, D-TA COF film/ITO electrodes exhibit significantly enhanced photocurrent and improved stability when compared with the randomly oriented D-TA COF powder drop-coated on ITO. After coupling with catalase (CAT), O_2 as an electron donor was introduced *in situ* due to the outstandingly catalytic activity of CAT toward H_2O_2. As a result, the photocurrent response was further improved (Scheme 1B). Based on the excellent photoelectric properties and dual amplified signal, the fabricated PEC bioanalysis format exhibits rapid response, high stability, and a wide linear range for H_2O_2 monitoring. In addition, the bioanalysis format also has excellent selectivity against potential interferences.

2. EXPERIMENTAL SECTION

2.1. Reagents and Apparatus. Tris(4-aminophenyl)amine (TAPA, 97%) and tetrabutylammonium hexafluorophosphate (Bu_4NPF_6) were obtained from Shanghai Xianding Biotechnology Co., Ltd. 2,6-Dihydroxynaphthalene-1,5-dicarbaldehyde (DHNDA) was prepared as reported in the literature.[43] Catalase (CAT, from bovine liver, 2000−5000 U/mg) and tris(hydroxymethyl) aminomethane (Tris) were purchased from Yuanye Biotech Co., Ltd. (Shanghai, China). Hydrogen peroxide solution (H_2O_2, 30%) was supplied by Sinopharm Chemical Reagent Co. Ltd. (Shanghai, China). Phorbol-12-myristate-13-acetate (PMA) was obtained from Beijing Solarbio Science & Technology Co., Ltd. (China). Indium tin oxide (ITO) glasses were purchased from Zhuhai Kaivo Optoelectronic Technology Co., Ltd. (China).

The powder X-ray diffraction (PXRD) pattern was measured on the PANalytical X'perts powder diffractometer. Scanning electron microscope (SEM) images were recorded on a field emission scanning electron microscope (FE-SEM SU8010). The atomic force microscope (AFM) images were obtained on a Bruker multimode 8. The UV−vis absorption spectrum was collected on an Agilent Cary 5000 UV−vis spectrophotometer. Raman spectra were obtained on a JY LABRAM-HR confocal micro-Raman spectrometer with a 633 nm laser source. X-ray photoelectron spectroscopy (XPS) experiments were performed on an ESCALAB 250 Xi spectrometer (Thermo Fisher Scientific, USA). Molecular models were constructed in the Materials Studio (MS). Two probable structures, a fully eclipsed model with an AA stacking sequence and a staggered model with an AB stacking sequence, were simulated. Simulations of the AA stacking sequence used a monoclinic unit cell ($P6/m$) with parameters of $a = b = 33.899$ Å, $c = 8.852$ Å, $\alpha = \beta = 90°$, and $\gamma = 120°$. Transmission electron microscope (TEM) images were measured on a JEOL JEM-1011 transmission electron microscope.

2.2. Synthesis of D-TA COF Films on ITO. DHNDA (1 mg) and TAPA (1 mg) were separately dissolved in a mixed solution containing mesitylene, ethanol, and acetic acid (v/v/v 5:5:1, 550 μL). Then the DHNDA and TAPA were mixed together at a volume ratio of 1:1. After that, 20 μL of the mixed solution was immediately dripped onto the ITO (1 cm × 2 cm) surface and kept at room temperature for 10 min in a closed system. Next, ITO glasses were submerged in methylene chloride for 5 min to remove the unreacted residues and dried at room temperature to obtain a uniform thin rosy-brown-colored film on the surface of the ITO.

2.3. Fabrication of the PEC Biosensor. Before electrode preparation, the ITO electrodes (1 cm × 2 cm) were ultrasonically washed with acetone, ethanol, and NaOH (1 M) in an ethanol/water mixed solution (v/v, 1:1) and ultrapure water for 15 min and dried by N_2. Then the D-TA COF film was modified on the ITO surface according to the procedure described above. After that, an insulation tape with a hollow-carved circle (0.4 cm in diameter) and conductive

https://dx.doi.org/10.1021/acsami.0c15147
ACS Appl. Mater. Interfaces XXXX, XXX, XXX−XXX

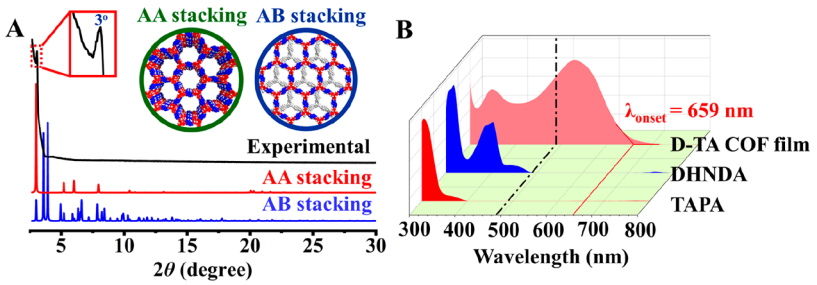

Figure 2. (A) Experimental (black), simulated AA stacking (red), and simulated AB stacking (blue) powder X-ray diffraction patterns for the D-TA COF film; (inset) illustration of the AA and AB stacking models for D-TA COF film. (B) UV−vis spectra of DHNDA and TAPA and UV−vis diffuse reflectance spectra of the D-TA COF film.

copper foil tape were pasted on the D-TA COF film/ITO, as shown in Figure S1.

The D-TA COF film modified electrode was incubated in 15 μL of catalase (CAT) solution (2.5 mg/mL) in a moisture-saturated environment for 60 min at room temperature to prevent evaporation of the solvent. Then, the resulting modified electrode was washed with Tris-HCl (10 mM, pH 7.4) to remove excessive CAT. The electrode was denoted as CAT/D-TA COF film/ITO and kept at 4 °C for further use.

Prior to the detection of H_2O_2, the supporting electrolyte solution was bubbled with a high concentration of pure nitrogen for 30 min to remove dissolved oxygen. Then the CAT/D-TA COF film/ITO electrodes were immersed in 20 mL of electrolyte solution containing a certain concentration of H_2O_2, and the photocurrents were measured 5 min later.

2.4. Photoelectrochemical Detection. PEC measurements were performed on a CHI 760C electrochemical workstation (Shanghai Chenhua Instrument Co., Ltd., China) with a common three-electrode system consisting of a modified ITO with a geometrical circular area (0.4 cm in diameter) as the working electrode, a platinum (Pt) sheet as a counter electrode, and a saturated calomel electrode (SCE) as a reference electrode under irradiation of a 500 W Xe lamp with an applied potential of 0 V. The supporting electrolyte solution was Tris-HCl buffer solution (10 mM, pH 7.4).

3. RESULTS AND DISCUSSION

3.1. Synthesis and Characterizations of the D-TA COF Film. The selection and preparation of photoelectric active materials are closely related to their PEC sensing performance. To obtain a stable photocurrent density, an ideal photoelectric active electrode should possess high stability, repeatability, easy fabrication, and a low electron−hole recombination rate. In this work, the *in situ* growth of D-TA COF thin film was synthesized via a Schiff base co-condensation reaction between DHNDA and TAPA monomers under very simple and mild conditions within a few minutes (Scheme 1A). The reaction can easily take place without high temperature, high pressure, or the addition of metal catalysts. The formed thin film was rosy-brown and shiny with a homogeneous topography and high crystallinity (inset of Scheme 1A). The film was transparent, and the lines of ITO could be clearly observed through the film, suggesting that the formed film was ultrathin. The other three COF films (BP-TA COF, P-TA COF, and D-TB COF) were also fabricated with the same concentration of 4,4′-biphenyldicarboxaldehyde and TAPA, or 1,4-phthalaldehyde and TAPA, or DHNDA and 1,3,5-tris(4-aminophenyl)-benzene (TAPB) by using the same synthesis method, respectively (Figure S2). The films presented different colors and were as homogeneous and translucent as the D-TA COF film. The results pointed out the feasibility and general applicability of the method to generate the *in situ* growth of COF thin films on ITO.

The successful preparation of D-TA COF thin film was confirmed by Raman spectroscopy and X-ray photoelectron spectroscopy (XPS) spectra. As revealed in Figure 1A, the bands at 1307 and 1697 cm^{-1} corresponded to the stretching and wagging vibration of NH_2 in TAPA and −CHO stretching vibrations in DHNDA, respectively.[44] However, these two bands remarkably decreased in the Raman spectrum of D-TA COF film. Also, a new band emerged at 1595 cm^{-1}, which corresponds to the C═N bonds, clearly indicating the successful condensation of DHNDA and TAPA by the Schiff base reaction.[45] The compositions of the film were further investigated by XPS. Figure S3 shows the presence of C, N, and O elements in the D-TA COF film. In the high-resolution XPS spectra of C 1s (Figure 1B), a clear emission line at a binding energy of 285.7 eV was detected, which was attributed to the C═N bonds.[46] The C═N bonds at 398.8 eV were also observed in the high-resolution XPS spectra of N 1s (Figure 1C).[47,48] These results were consistent with that observed in the Raman spectra, further confirming the formation of the imine linkers in the D-TA COF thin film.

The morphologies of the D-TA COF thin film were next characterized by SEM, TEM, and AFM. The top-view SEM image shows a continuous and homogeneous film covering the ITO surface (Figure 1D). The boundary between the film and ITO was hardly distinguished from the SEM cross section (Figure 1E), which confirms that the film was ultrathin and strongly adhered on the ITO surface. The almost zero distance contact allows the electric charges to conveniently shuttle between the film and ITO without hindrance, thereby effectively improving the electron transmission efficiency and in turn the PEC sensing performance. When the film grew on the carbon-coated copper grid, an ultrathin sheetlike film was observed (Figure 1F). Its thickness was about several nanometers. From the AFM image, we also found that the thickness of the film fluctuated within 10 nm (Figure 1H) with a root-mean-square (rms) roughness value of 2.47 nm, once again implying that the film formed is ultrathin. The film on the ITO was uniform when observed with the naked eye. However, the surface of the film was uneven from the AFM and TEM images (Figures 1I and 1G) due to the large number of pores formed by the oriented growth of the D-TA COF film. This as well as the extended π-conjugated frameworks would be of benefit for the following large amount of coupling and embeddedness of the CAT enzyme, which provided the basis for PEC biosensor design. Clearly, this strategy to fabricate electrodes is facile and environmentally friendly, not needing the modification of extra materials, such as chitosan and

https://dx.doi.org/10.1021/acsami.0c15147
ACS Appl. Mater. Interfaces XXXX, XXX, XXX−XXX

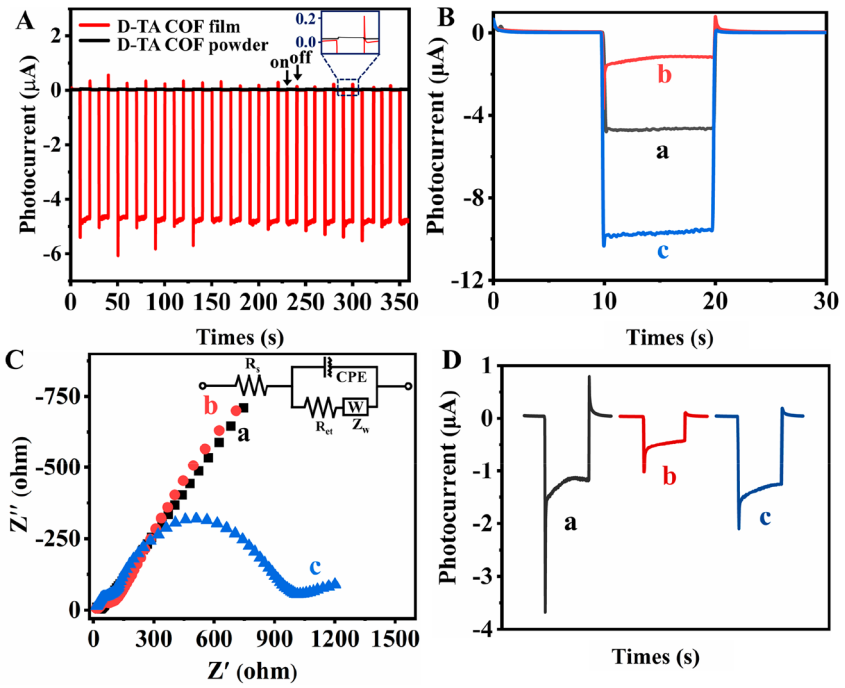

Figure 3. (A) Photocurrent responses of D-TA COF film/ITO (red) and D-TA COF powder/ITO in 10 mM air-saturated Tris-HCl buffer solution. (B) Photocurrent responses of D-TA COF film/ITO in (a) air-saturated, (b) N_2-saturated, and (c) O_2-saturated Tris-HCl buffer solution. (C) EIS Nyquist plots of (a) bare ITO, (b) D-TA COF film/ITO, and (c) CAT/D-TA COF film/ITO. The inset is the Randles equivalent circuit for EIS. (D) Photocurrent responses of (a) D-TA COF film/ITO, (b) CAT/D-TA COF film/ITO in N_2-saturated Tris-HCl buffer solution, and (c) CAT/D-TA COF film/ITO in N_2-saturated Tris-HCl buffer solution with 1 mM H_2O_2.

poly(diallyldimethylammonium chloride) (PDDA) to provide additional interaction forces.[49−51]

Powder X-ray diffraction (PXRD) analysis was performed to evaluate the degree of crystallinity of the D-TA COF film on the ITO. The experimental PXRD pattern of D-TA COF film had a main peak at 3.0° with a *d* spacing of 29.45 Å, corresponding to the refractions from the (010) plane, indicating the long-range orderliness of molecular stacking in the film (Figure 2A, black line). Also, the Materials Studio software package was utilized to analyze the lattice modeling of the D-TA COF film. As can be seen, the experimental diffraction peak is consistent with the simulated peak of the AA stacking model, indicating that the D-TA COF film prefers to form a regular ordered and fully eclipsed layered-sheet arrangement. Medina et al. prepared oriented thin films on ITO under high temperature and pressure.[24] Some two-dimensional covalent organic frameworks have also been fabricated at liquid−liquid interfaces.[14,27,52] However, in the present case, the regular ordered thin film can be obtained based on the *in situ* growth on ITO under room temperature, which makes it a suitable candidate for PEC biosensor practical application.

3.2. UV−Vis Absorption and Electrochemical Properties of the D-TA COF Film. To obtain the light absorption ability of D-TA COF film, the electronic performance of the material was assessed by ultraviolet−visible diffuse reflectance spectroscopy (Figure 2B). Compared with DHNDA and TAPA monomers, which only display narrow maximum absorption peaks at 317, 403, and 305 nm, respectively, the D-TA COF thin film has a significantly broader and stronger absorption band in the range of 300−600 nm, and the absorption tail even extends beyond 700 nm. These results indicate that the periodic and highly conjugated frameworks of D-TA COF could benefit the π electrons delocalization and ordered stacking of D-TA COF layers. This in turn could further enhance its light harvesting capability in a wide visible light region. Such strong absorption makes the D-TA COF film a good choice as an efficient photoelectric conversion material. Based on the onset absorption wavelength (λ_{onset}) by the formula $E_g = 1240/\lambda_{onset}$, the optical band gap ($E_g$) was calculated to be 1.88 eV. Such a small band gap also implies the π electrons delocalization over the D-TA COF film, which benefits the generation of more charge carriers after absorbing photons, leading to higher photoelectric conversion efficiency. Next, the energy levels of the lowest unoccupied molecular orbital (LUMO) and the highest occupied molecular orbital (HOMO) of the D-TA COF film were estimated by cyclic voltammetry (CV) measurement according to the following formulas: $E_{HOMO} = -(4.8\ eV - E_{1/2}^{Fc/Fc+} + E_{ox})$ and $E_{LUMO} = E_{HOMO} + E_g$. As shown in Figure S4, the onset oxidation position (E_{ox}) of the D-TA COF film was −0.12 V. Thus, the E_{HOMO} was calculated as −4.71 eV. Then, the E_{LUMO} of −2.83 eV was obtained.

3.3. PEC Activity of D-TA COF Film. The photocurrent response of the D-TA COF film on the ITO electrode in Tris-HCl buffer solution (pH 7.4) was investigated under radiation from an Xe lamp at a bias potential of 0 V. The results are shown in Figure 3A. The D-TA COF film had a sensitive response to light irradiation and generated a strong cathodic photocurrent of ca. −4.6 μA. In addition, the photocurrent response of the D-TA COF film on ITO was stable, which was revealed by repeating on/off irradiation cycles for 350 s, which indicated that the D-TA COF film possessed superior PEC activity for bioanalysis and biosensors. However, a photocurrent of ca. 15 nA was observed for the D-TA COF powder drop-coated ITO electrode (black line in Figure 3A). The D-

https://dx.doi.org/10.1021/acsami.0c15147
ACS Appl. Mater. Interfaces XXXX, XXX, XXX−XXX

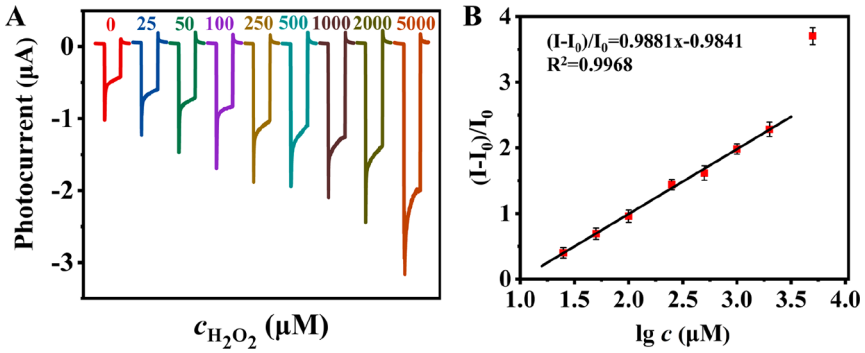

Figure 4. (A) Photocurrent responses of the CAT/D-TA COF film/ITO electrodes to H_2O_2 with different concentrations. (B) The corresponding calibration curve of photocurrent change and the logarithm of H_2O_2 concentrations.

TA COF powder was obtained by scraping the *in situ* growth D-TA COF film from the ITO surface. Compared with the randomly oriented D-TA COF powder, the photocurrent of the D-TA COF film grown on the ITO surface *in situ* achieved as high as ~333-fold increase, attributed to its closer distance and fewer interface defects between the photoactive material and the electrode, crystallinity, and a more regular ordered stacking mode. Furthermore, when the D-TA COF film/ITO electrode was continually immersed in Tris-HCl buffer solution for 90 min, no obvious change in the photocurrent response was observed (Figure S5). This result indicates no leaching of the D-TA COF film from ITO happened, further revealing the stability of the D-TA COF film on the ITO electrode.

To investigate the photocatalytic mechanism, the photocurrent responses of the D-TA COF film in N_2-saturated and O_2-saturated Tris-HCl buffer solution were tested (Figure 3B). When the buffer solution was deoxygenated by highly pure N_2, the photocurrent response of the D-TA COF film decreased to −1.1 μA (curve b). However, the photocurrent response significantly increased to −9.5 μA under an O_2-saturated buffer solution (curve c). The results indicated that the photocurrent response of the D-TA COF film was sensitive to dissolved oxygen. According to the obtained energy level values as detailed above, the speculated electron transfer process is depicted in Scheme 1C. Under light irradiation, the D-TA COF film harvested high-energy photons, leading to the transfer of photogenerated electrons from the HOMO to the LUMO of D-TA COF and in turn generating electron−hole pairs. Subsequently, electrons could transfer to the electron acceptors (O_2 molecules) in the electrolyte solution, since the reduction potential of oxygen was lower than the LUMO of the D-TA COF film,[53] while the photogenerated holes formed on the HOMO were captured by the ITO electrode. The process effectively inhibited electron−hole pair recombination of the D-TA COF film, resulting in the generation of a stable and strong cathodic photocurrent.

3.4. Characterizations and Feasibility of the Designed Biosensor. The D-TA COF film on ITO was coupled with CAT, and the fabricated electrode was denoted as CAT/D-TA COF film/ITO. To verify the PEC biosensor's successful construction, electrochemical impedance spectroscopy (EIS) and PEC response of the ITO electrodes at different stages were estimated. EIS measurements were performed in 0.1 M KCl containing 5.0 mM $K_3[Fe(CN)_6]$/$K_4[Fe(CN)_6]$ (1:1) over a frequency range from 10 kHz to 0.01 Hz by using an alternative voltage with an amplitude of 5 mV (Figure 3C). The inset in Figure 3C is the Randles equivalent circuit simulated with Zview software, whose fitting curves are presented in Figure S6. When the ITO was modified with the D-TA COF thin film, the electron transfer resistance (R_{et}) slightly increased to 62 Ω. This value is only a little worse than bare ITO, indicating the excellent electrical conductivity of the *in situ* generated D-TA COF film. After assembling CAT on the D-TA COF film/ITO surface, the R_{et} significantly increased because the poor conductivity and steric hindrance of the protein molecules retarded the electron-transfer rate.

The fabrication process was further characterized by the corresponding PEC responses of different modified electrodes in N_2-saturated Tris-HCl buffer solution (Figure 3D). When the D-TA COF film/ITO surface was modified with CAT, the photocurrent response significantly decreased, which was consistent with EIS results. In the presence of 1 mM H_2O_2, the photocurrent response increased ~840 nA because of the effective catalytic decomposition of H_2O_2 into O_2 by CAT. This result also validated the dual-signal amplification, namely, the effect of the intrinsic catalytic property of CAT synergized with the good response of the D-TA COF film/ITO for O_2, which further guarantees enough sensitivity to detect hydrogen peroxide released from living cells. In conclusion, from the variations of R_{et} and the photocurrent response of the stepwise-modified procedure, the successful fabrication of the PEC biosensor was revealed.

3.5. Optimization of the Experimental Conditions. To obtain a PEC biosensor with high sensitivity toward H_2O_2, we optimized the experimental conditions such as the concentration of CAT, the incubation time of CAT, and the reaction time of the electrode in electrolyte containing H_2O_2. As seen from Figure S7A, the photocurrent increased with an increase of the concentration of CAT from 0.5 to 2.5 mg/mL and then declined at 3.0 mg/mL, possibly because too much CAT on the electrode hindered the light absorption of the D-TA COF film and the electron transfer. Thus, 2.5 mg/mL was employed as the optimal concentration of CAT. The photocurrent was promoted with the incubation time of CAT and the reaction time of the electrode in electrolyte containing H_2O_2 and tended to level off after 60 and 5 min, respectively (Figure S7B,C). Hence, the optimized incubation time of CAT and reaction time of the electrode in electrolyte containing H_2O_2 were 60 and 5 min, respectively.

3.6. PEC Analysis Performance for H_2O_2. Under optimized conditions, the analytic function of the as-proposed PEC biosensor was evaluated by detecting H_2O_2 of different concentrations, and the results are presented in Figure 4A. As

https://dx.doi.org/10.1021/acsami.0c15147
ACS Appl. Mater. Interfaces XXXX, XXX, XXX−XXX

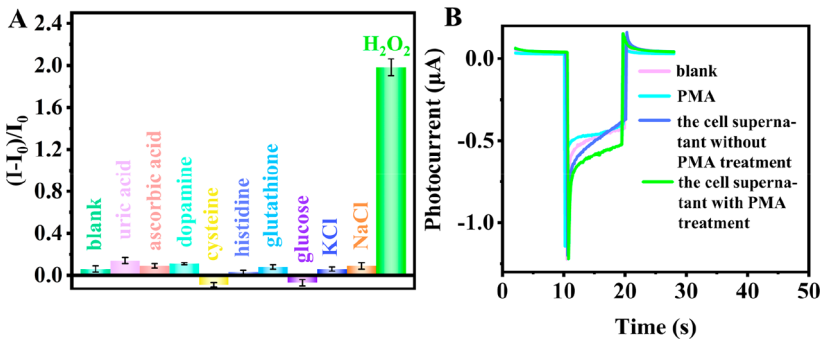

Figure 5. (A) Selectivity of the PEC biosensor for H_2O_2 detection. (B) The proposed PEC biosensor was applied to detect H_2O_2 released from HeLa cells.

expected, the intensity of the photocurrent enhanced accordingly with the concentrations of H_2O_2 increasing from 25 μM to 5 mM. As shown in Figure 4B, the calibration plot had a good linear relationship between the percentage of the photocurrent increase and the logarithm of the H_2O_2 concentration (log c) ranging from 25 μM to 2 mM, fitted as $(I - I_0)/I_0 = 0.9881 \log c - 0.9841$ with a correlation coefficient (R^2) of 0.9968. The limit of detection (LOD) was calculated to be 1.91 μM according to the calculation of 3 times the standard deviation of background signal. In addition, the detection property of the proposed PEC biosensor was compared to some recent biosensor for H_2O_2 detection (Table S1). As can be seen, a wider linear range and a comparable or lower LOD were observed in our work, which were mainly attributed to the excellent PEC property of the D-TA COF film as well as the excellent catalytic property of CAT.

3.7. Selectivity, Reproducibility, and Long-Term Stability of the H_2O_2 Biosensor. To explore the selectivity of the PEC biosensor, the photocurrent responses of the CAT/D-TA COF film/ITO electrodes to some common species in human beings, such as amino acids (cysteine, histidine, and glutathione), inorganic salts (KCl and NaCl), uric acid, ascorbic acid, dopamine, and glucose, were recorded under the same conditions (Figure 5A). As a result, only H_2O_2 caused an obvious PEC current enhancement, and the interfering substances showed little influence. The good selectivity could be ascribed not only to the efficient selectivity of the natural enzyme for substrates but also to the cathodic PEC system which has strong anti-interference capability against reducing substances, providing the potential for application in real samples.[50] In addition, the reproducibility of the biosensor was investigated by assaying 1 mM H_2O_2 with five independently constructed biosensors, and the relative standard deviation (RSD) was 4.9%, implying the satisfactory reproducibility. To investigate the stability, the modified electrode was stored at 4 °C for 7 days. The photocurrent response still retained 93%, which indicated the excellent stability of the biosensor.

3.8. Application to Extracellular H_2O_2 Released from Living Cells. To validate the practical application of the proposed PEC biosensor for real biological sample detection, H_2O_2 released from living cells was measured. The cell line of human cervical cancer (HeLa) was selected as model cells in this work. Phorbol 12-myristate 13-acetate (PMA) was used to stimulate the generation of H_2O_2 in HeLa cells.[33] First, the HeLa cells were dispersed in N_2-saturated PBS. Then PMA (20 ng mL^{-1}) was added into the cell suspensions, followed by centrifugation. The supernatant was added in the electrolyte for the PEC test, and the results are shown in Figure 5B. A significant increased photocurrent was recorded after adding the above supernatant. However, no obvious current changes in the cases of adding PMA or the supernatant without treatment with PMA were found, thus indicating that the increased photocurrent came from O_2 produced by the catalytic decomposition of H_2O_2 released from the living cells. The experiment was repeated five times, and the photocurrent responses offered a RSD of 7.1%, which confirmed a satisfactory reproducibility in detection H_2O_2 released from the living cells. The results indicated that the established PEC platform possessed great potential to monitor H_2O_2 released from living cells due to its dual catalytic amplification and ultrahigh sensitivity.

4. CONCLUSIONS

In summary, we successfully fabricated COF film-based PEC electrodes (D-TA COF film/ITO) under very simple and mild conditions within a few minutes. COF films were synthesized *in situ* on the ITO surface by a Schiff-base co-condensation reaction with almost complete surface coverage and a thickness of several nanometers. Its well-defined, crystalline-oriented structure was revealed by PXRD characterization. The obtained D-TA COF/ITO electrodes as expected possess significantly enhanced photocurrent and improved stability. The porous structure and open channels of the D-TA COF film afford a perfect architecture for coupling with large amounts of CAT molecules. Based on the unique photoelectric property, high conductivity, and the outstanding catalytic ability of CAT toward H_2O_2, a D-TA COF film-based PEC biosensor was established with good sensitivity, rapid response, and high stability. This study contributes an original prototype to construct COF film-based PEC electrodes with excellent performance, demonstrating the great potential of versatile COF films in future PEC bioanalysis application.

■ ASSOCIATED CONTENT

Supporting Information

The Supporting Information is available free of charge at https://pubs.acs.org/doi/10.1021/acsami.0c15147.

Cell cultures and detection extracellular H_2O_2 released from living cells; photographs of electrode; the other three COF films preparation; XPS survey spectrum; CV curves; photocurrent response of D-TA COF film/ITO electrode after immersing in Tris-HCl buffer solution for 90 min; optimization condition; comparison of the reported strategy for H_2O_2 detection (PDF)

https://dx.doi.org/10.1021/acsami.0c15147
ACS Appl. Mater. Interfaces XXXX, XXX, XXX−XXX

AUTHOR INFORMATION

Corresponding Authors

Lin Cui − *College of Chemistry, Chemical Engineering and Materials Science, Shandong Normal University, Jinan, Shandong 250014, China*; Email: zhangxiaomei@sdu.edu.cn

Xiaomei Zhang − *School of Chemistry and Chemical Engineering, Shandong University, Jinan, Shandong 250100, China*; orcid.org/0000-0001-9056-5133; Email: zpbzcl@126.com

Authors

Tingting Liu − *School of Chemistry and Chemical Engineering, Shandong University, Jinan, Shandong 250100, China*

Huijuan Zhao − *School of Chemistry and Chemical Engineering, Shandong University, Jinan, Shandong 250100, China*

Complete contact information is available at: https://pubs.acs.org/10.1021/acsami.0c15147

Notes

The authors declare no competing financial interest.

ACKNOWLEDGMENTS

This work was supported by the National Natural Science Foundation of China (21977064 and 21974080), Shandong Provincial Key Research and Development Program (Major Scientific and Technological Innovation Project) (no. 2019JZZY010804), and the Scientific and Technological Projects of Shandong Province (2019GHY112028).

REFERENCES

(1) Zhao, W.; Xu, J.; Chen, H. Photoelectrochemical Immunoassays. *Anal. Chem.* **2018**, *90*, 615−627.

(2) Zhang, N.; Zhang, L.; Ruan, Y.; Zhao, W.; Xu, J.; Chen, H. Quantum-dots-based photoelectrochemical bioanalysis highlighted with recent examples. *Biosens. Bioelectron.* **2017**, *94*, 207−218.

(3) Peng, J.; Huang, Q.; Zhuge, W.; Liu, Y.; Zhang, C.; Yang, W.; Xiang, G. Blue-light photoelectrochemical sensor based on nickel tetra-amined phthalocyanine-graphene oxide covalent compound for ultrasensitive detection of erythromycin. *Biosens. Bioelectron.* **2018**, *106*, 212−218.

(4) Zhao, W.; Xu, J.; Chen, H. Photoelectrochemical bioanalysis: the state of the art. *Chem. Soc. Rev.* **2015**, *44*, 729−741.

(5) Hu, T.; Zheng, Y.; Li, M.; Liang, W.; Chai, Y.; Yuan, R. A Highly Sensitive Photoelectrochemical Assay with Donor-Acceptor-Type Material as Photoactive Material and Polyaniline as Signal Enhancer. *Anal. Chem.* **2018**, *90*, 6096−6101.

(6) Li, F.; Wang, S.; Yin, H.; Chen, Y.; Zhou, Y.; Huang, J.; Ai, S. Photoelectrochemical Biosensor for DNA Formylation Detection in Genomic DNA of Maize Seedlings Based on Black TiO_2-Enhanced Photoactivity of MoS_2/WS_2 Heterojunction. *ACS Sens.* **2020**, *5*, 1092−1101.

(7) Zhang, Y.; Li, M.; Wang, H.; Yuan, R.; Wei, S. Supersensitive Photoelectrochemical Aptasensor Based on Br,N-Codoped TiO_2 Sensitized by Quantum Dots. *Anal. Chem.* **2019**, *91*, 10864−10869.

(8) Li, P.; Cao, Y.; Mao, C.; Jin, B.; Zhu, J. TiO_2/g-C_3N_4/CdS Nanocomposite-Based Photoelectrochemical Biosensor for Ultrasensitive Evaluation of T4 Polynucleotide Kinase Activity. *Anal. Chem.* **2019**, *91*, 1563−1570.

(9) Sun, B.; Dong, J.; Cui, L.; Feng, T.; Zhu, J.; Liu, X.; Ai, S. A dual signal-on photoelectrochemical immunosensor for sensitively detecting target avian viruses based on AuNPs/g-C_3N_4 coupling with CdTe quantum dots and in situ enzymatic generation of electron donor. *Biosens. Bioelectron.* **2019**, *124*−*125*, 1−7.

(10) Peng, J.; Huang, Q.; Liu, Y.; Liu, P.; Zhang, C. Photoelectrochemical sensor based on composite of CdTe and nickel tetra-amined phthalocyanine covalently linked with graphene oxide for ultrasensitive detection of curcumin. *Sens. Actuators, B* **2019**, *294*, 157−165.

(11) Peng, J.; Zhuge, W.; Liu, Y.; Zhang, C.; Yang, W.; Huang, Y. Photoelectrochemical Dopamine Sensor Based on Cu-Doped Bi_2WO_6 Micro-Flowers Sensitized Cobalt Tetraaminophthalocyanine Functionalized Graphene Oxide. *J. Electrochem. Soc.* **2019**, *166*, B1612−B1619.

(12) Zhao, W.; Xu, J.; Chen, H. Photoelectrochemical enzymatic biosensors. *Biosens. Bioelectron.* **2017**, *92*, 294−304.

(13) Bai, L.; Phua, S. Z. F.; Lim, W. Q.; Jana, A.; Luo, Z.; Tham, H. P.; Zhao, L.; Gao, Q.; Zhao, Y. Nanoscale covalent organic frameworks as smart carriers for drug delivery. *Chem. Commun.* **2016**, *52*, 4128−4131.

(14) Dey, K.; Pal, M.; Rout, K. C.; Kunjattu, H. S.; Das, A.; Mukherjee, R.; Kharul, U. K.; Banerjee, R. Selective Molecular Separation by Interfacially Crystallized Covalent Organic Framework Thin Films. *J. Am. Chem. Soc.* **2017**, *139*, 13083−13091.

(15) Jiang, L.; Tian, Y.; Sun, T.; Zhu, Y.; Ren, H.; Zou, X.; Ma, Y.; Meihaus, K. R.; Long, J. R.; Zhu, G. A Crystalline Polyimide Porous Organic Framework for Selective Adsorption of Acetylene over Ethylene. *J. Am. Chem. Soc.* **2018**, *140*, 15724−15730.

(16) Doonan, C. J.; Tranchemontagne, D. J.; Glover, T. G.; Hunt, J. R.; Yaghi, O. M. Exceptional ammonia uptake by a covalent organic framework. *Nat. Chem.* **2010**, *2*, 235−238.

(17) Ding, S.; Gao, J.; Wang, Q.; Zhang, Y.; Song, W.; Su, C.; Wang, W. Construction of Covalent Organic Framework for Catalysis: Pd/COF-LZU1 in Suzuki-Miyaura Coupling Reaction. *J. Am. Chem. Soc.* **2011**, *133*, 19816−19822.

(18) Fang, Q.; Gu, S.; Zheng, J.; Zhuang, Z.; Qiu, S.; Yan, Y. 3D Microporous Base-Functionalized Covalent Organic Frameworks for Size-Selective Catalysis. *Angew. Chem., Int. Ed.* **2014**, *53*, 2878−2882.

(19) Zhang, T.; Ma, N.; Ali, A.; Wei, Q.; Wu, D.; Ren, X. Electrochemical ultrasensitive detection of cardiac troponin I using covalent organic frameworks for signal amplification. *Biosens. Bioelectron.* **2018**, *119*, 176−181.

(20) Zhao, Y.; Dai, W.; Peng, Y.; Niu, Z.; Sun, Q.; Shan, C.; Yang, H.; Verma, G.; Wojtas, L.; Yuan, D.; Zhang, Z.; Dong, H.; Zhang, X.; Zhang, B.; Feng, Y.; Ma, S. A Corrole-Based Covalent Organic Framework Featuring Desymmetrized Topology. *Angew. Chem., Int. Ed.* **2020**, *59*, 4354−4359.

(21) Wang, Y.; Liu, H.; Pan, Q.; Wu, C.; Hao, W.; Xu, J.; Chen, R.; Liu, J.; Li, Z.; Zhao, Y. Construction of Fully Conjugated Covalent Organic Frameworks via Facile Linkage Conversion for Efficient Photoenzymatic Catalysis. *J. Am. Chem. Soc.* **2020**, *142*, 5958−5963.

(22) Wan, G.; Fu, Y.; Guo, J.; Xiang, Z. Photoelectronic Porous Covalent Organic Materials: Research Progress and Perspective. *Huaxue Xuebao* **2015**, *73*, 557−578.

(23) Rotter, J. M.; Weinberger, S.; Kampmann, J.; Sick, T.; Shalom, M.; Bein, T.; Medina, D. D. Covalent Organic Framework Films through Electrophoretic Deposition-Creating Efficient Morphologies for Catalysis. *Chem. Mater.* **2019**, *31*, 10008−10016.

(24) Medina, D. D.; Werner, V.; Auras, F.; Tautz, R.; Dogru, M.; Schuster, J.; Linke, S.; Döblinger, M.; Feldmann, J.; Knochel, P.; Bein, T. Oriented Thin Films of a Benzodithiophene Covalent Organic Framework. *ACS Nano* **2014**, *8*, 4042−4052.

(25) Li, Y.; Chen, Q.; Xu, T.; Xie, Z.; Liu, J.; Yu, X.; Ma, S.; Qin, T.; Chen, L. De Novo Design and Facile Synthesis of 2D Covalent Organic Frameworks: A Two-in-One Strategy. *J. Am. Chem. Soc.* **2019**, *141*, 13822−13828.

(26) Xu, L.; Zhou, X.; Yu, Y.; Tian, W. Q.; Ma, J.; Lei, S. Surface-Confined Crystalline Two-Dimensional Covalent Organic Frameworks via on-Surface Schiff-Base Coupling. *ACS Nano* **2013**, *7*, 8066−8073.

(27) Li, C.; Wang, Y.; Zou, Y.; Zhang, X.; Dong, H.; Hu, W. Two-Dimensional Conjugated Polymer Synthesized by Interfacial Suzuki Reaction: Towards Electronic Device Applications. *Angew. Chem., Int. Ed.* **2020**, *59*, 9403−9407.

(28) Jin, P.; Niu, X.; Zhang, F.; Dong, K.; Dai, H.; Zhang, H.; Wang, W.; Chen, H.; Chen, X. Stable and Reusable Light-Responsive

Reduced Covalent Organic Framework (COF-300-AR) as a Oxidase-Mimicking Catalyst for GSH Detection in Cell Lysate. *ACS Appl. Mater. Interfaces* **2020**, *12*, 20414−20422.
(29) Hai, J.; Wang, H.; Sun, P.; Li, T.; Lu, S.; Zhao, Y.; Wang, B. Smart Responsive Luminescent Aptamer-Functionalized Covalent Organic Framework Hydrogel for High-Resolution Visualization and Security Protection of Latent Fingerprints. *ACS Appl. Mater. Interfaces* **2019**, *11*, 44664−44672.
(30) Zhang, C.; Zhang, S.; Yan, Y.; Xia, F.; Huang, A.; Xian, Y. Highly Fluorescent Polyimide Covalent Organic Nanosheets as Sensing Probes for the Detection of 2,4,6-Trinitrophenol. *ACS Appl. Mater. Interfaces* **2017**, *9*, 13415−13421.
(31) Yan, X.; Song, Y.; Liu, J.; Zhou, N.; Zhang, C.; He, L.; Zhang, Z.; Liu, Z. Two-dimensional porphyrin-based covalent organic framework: A novel platform for sensitive epidermal growth factor receptor and living cancer cell detection. *Biosens. Bioelectron.* **2019**, *126*, 734−742.
(32) Zhang, X.; Chi, K.; Li, D.; Deng, Y.; Ma, Y.; Xu, Q.; Hu, R.; Yang, Y. 2D-porphrinic covalent organic framework-based aptasensor with enhanced photoelectrochemical response for the detection of C-reactive protein. *Biosens. Bioelectron.* **2019**, *129*, 64−71.
(33) Du, H.; Zhang, X.; Liu, Z.; Qu, F. A supersensitive biosensor based on MoS_2 nanosheet arrays for the real-time detection of H_2O_2 secreted from living cells. *Chem. Commun.* **2019**, *55*, 9653−9656.
(34) Shu, X.; Chen, Y.; Yuan, H.; Gao, S.; Xiao, D. H_2O_2 Sensor Based on the Room-Temperature Phosphorescence of Nano TiO_2/SiO_2 Composite. *Anal. Chem.* **2007**, *79*, 3695−3702.
(35) Pramanik, D.; Dey, S. G. Active Site Environment of Heme-Bound Amyloid β Peptide Associated with Alzheimer's Disease. *J. Am. Chem. Soc.* **2011**, *133*, 81−87.
(36) Houstis, N.; Rosen, E. D.; Lander, E. S. Reactive oxygen species have a causal role in multiple forms of insulin resistance. *Nature* **2006**, *440*, 944−948.
(37) Wei, Y.; Zhang, Y.; Liu, Z.; Guo, M. A novel profluorescent probe for detecting oxidative stress induced by metal and H_2O_2 in living cells. *Chem. Commun.* **2010**, *46*, 4472−4474.
(38) Deng, W.; Peng, Y.; Yang, H.; Tan, Y.; Ma, M.; Xie, Q.; Chen, S. Ruthenium Ion-Complexed Carbon Nitride Nanosheets with Peroxidase-like Activity as a Ratiometric Fluorescence Probe for the Detection of Hydrogen Peroxide and Glucose. *ACS Appl. Mater. Interfaces* **2019**, *11*, 29072−29077.
(39) Cui, C.; Wang, Q.; Liu, Q.; Deng, X.; Liu, T.; Li, D.; Zhang, X. Porphyrin-based porous organic framework: An efficient and stable peroxidase-mimicking nanozyme for detection of H_2O_2 and evaluation of antioxidant. *Sens. Actuators, B* **2018**, *277*, 86−94.
(40) Zhang, T.; Xing, Y.; Song, Y.; Gu, Y.; Yan, X.; Lu, N.; Liu, H.; Xu, Z.; Xu, H.; Zhang, Z.; Yang, M. AuPt/MOF−Graphene: A Synergistic Catalyst with Surprisingly High Peroxidase-Like Activity and Its Application for H_2O_2 Detection. *Anal. Chem.* **2019**, *91*, 10589−10595.
(41) Balasubramanian, P.; Annalakshmi, M.; Chen, S.; Sathesh, T.; Peng, T.; Balamurugan, T. S. T. Facile Solvothermal Preparation of Mn_2CuO_4 Microspheres: Excellent Electrocatalyst for Real-Time Detection of H_2O_2 Released from Live Cells. *ACS Appl. Mater. Interfaces* **2018**, *10*, 43543−43551.
(42) Li, R.; Zhang, Y.; Tu, W.; Dai, Z. Photoelectrochemical Bioanalysis Platform for Cells Monitoring Based on Dual Signal Amplification Using in Situ Generation of Electron Acceptor Coupled with Heterojunction. *ACS Appl. Mater. Interfaces* **2017**, *9*, 22289−22297.
(43) Houjou, H.; Motoyama, T.; Banno, S.; Yoshikawa, I.; Araki, K. Experimental and Theoretical Studies on Constitutional Isomers of 2,6-Dihydroxynaphthalene Carbaldehydes. Effects of Resonance-Assisted Hydrogen Bonding on the Electronic Absorption Spectra. *J. Org. Chem.* **2009**, *74*, 520−529.
(44) Sun, B.; Zhu, C.; Liu, Y.; Wang, C.; Wan, L.; Wang, D. Oriented Covalent Organic Framework Film on Graphene for Robust Ambipolar Vertical Organic Field-Effect Transistor. *Chem. Mater.* **2017**, *29*, 4367−4374.
(45) Dai, W.; Shao, F.; Szczerbiński, J.; McCaffrey, R.; Zenobi, R.; Jin, Y.; Schlüter, A. D.; Zhang, W. Synthesis of a Two-Dimensional Covalent Organic Monolayer through Dynamic Imine Chemistry at the Air/Water Interface. *Angew. Chem., Int. Ed.* **2016**, *55*, 213−217.
(46) Arul, P.; Narayanamoorthi, E.; John, S. A. Covalent organic framework film as an effective electrocatalyst for the simultaneous determination of dihydroxybenzene isomers in water samples. *Sens. Actuators, B* **2020**, *313*, 128033.
(47) Cheung, P. L.; Lee, S. K.; Kubiak, C. P. Facile Solvent-Free Synthesis of Thin Iron Porphyrin COFs on Carbon Cloth Electrodes for CO_2 Reduction. *Chem. Mater.* **2019**, *31*, 1908−1919.
(48) Meng, Z.; Stolz, R. M.; Mirica, K. A. Two-Dimensional Chemiresistive Covalent Organic Framework with High Intrinsic Conductivity. *J. Am. Chem. Soc.* **2019**, *141*, 11929−11937.
(49) Zhao, C.; Zhou, J.; Wu, K.; Ding, S.; Xu, J.; Chen, H. Plasmonic Enhanced Gold Nanoclusters-Based Photoelectrochemical Biosensor for Sensitive Alkaline Phosphatase Activity Analysis. *Anal. Chem.* **2020**, *92*, 6886−6892.
(50) Zhang, L.; Ruan, Y.; Liang, Y.; Zhao, W.; Yu, X.; Xu, J.; Chen, H. Bismuth Oxyiodide Couples with Glucose Oxidase: A Special Synergized Dual-Catalysis Mechanism for Photoelectrochemical Enzymatic Bioanalysis. *ACS Appl. Mater. Interfaces* **2018**, *10*, 3372−3379.
(51) Zhang, L.; Zhu, Y.; Liang, Y.; Zhao, W.; Xu, J.; Chen, H. Semiconducting CuO Nanotubes: Synthesis, Characterization, and Bifunctional Photocathodic Enzymatic Bioanalysis. *Anal. Chem.* **2018**, *90*, 5439−5444.
(52) Zhou, D.; Tan, X.; Wu, H.; Tian, L.; Li, M. Synthesis of C-C Bonded Two-Dimensional Conjugated Covalent Organic Framework Films by Suzuki Polymerization on a Liquid−Liquid Interface. *Angew. Chem., Int. Ed.* **2019**, *58*, 1376−1381.
(53) Li, C.; Lu, W.; Zhu, M.; Tang, B. Development of Visible-Light Induced Photoelectrochemical Platform Based on Cyclometalated Iridium (III) Complex for Bioanalysis. *Anal. Chem.* **2017**, *89*, 11098−11106.

https://dx.doi.org/10.1021/acsami.0c15147
ACS Appl. Mater. Interfaces XXXX, XXX, XXX−XXX